LWT - Food Science and Technology 160 (2022) 113335

Contents lists available at ScienceDirect

LWT

journal homepage: www.elsevier.com/locate/lwt

Thermodynamic analysis and modeling of water vapor adsorption isotherms of roasted specialty coffee (*Coffee arabica* L. cv. Colombia)

Gentil A. Collazos-Escobar [a,b], Nelson Gutiérrez-Guzmán [a], Henry A. Váquiro-Herrera [c], José Bon [b], José V. Garcia-Perez [b,*]

[a] Centro Surcolombiano de Investigación en Café CESURCAFÉ, Universidad Surcolombiana, Neiva-Huila, Colombia
[b] Grupo de Análisis y Simulación de Procesos Agroalimentarios (ASPA), Departamento de Tecnología de Alimentos, Universitat Politécnica de València, C/Cami de Vera S/n, 46022, Valencia, Spain
[c] Facultad de Ingeniería Agronómica, Universidad Del Tolima, Ibagué-Tolima, Colombia

ARTICLE INFO

Keywords:
Coffee wet processing
Hygroscopicity
ATR–FTIR
Gibbs free energy
Entropy

ABSTRACT

The experimental assessment and computer modeling of the water vapor adsorption isotherms of roasted specialty coffee is addressed in this study. Thus, both coffee beans and ground coffee of medium (850 μm) and fine (600 μm) particle sizes were analyzed over a range of water activities of between 0.1 and 0.9 and at temperatures of 25, 35, and 45 °C. The adsorption isotherms were determined using the dynamic dew point (DDI) method. The computer modeling of adsorption isotherms was addressed in order to describe the influence of the water activity and temperature on the equilibrium moisture content. Furthermore, the hygroscopic capacity of roasted coffee was analyzed by differential thermodynamic analysis. Experimental results and modeling showed that the high level of moisture adsorption found in the ground coffee was related to a large adsorption area, suggesting that specialty coffee should preferably be stored as beans. The Peleg empirical model was the most suitable at representing both type III upward concave adsorption behavior and the effect of temperature on the adsorption isotherms. Differential thermodynamic analysis revealed an increase in the water adsorption energy at low equilibrium moisture content, while negative Gibbs free energy values revealed the spontaneity of the adsorption process.

1. Introduction

Economically, coffee is one of the most important agricultural commodities and *Coffea arabica* dominates global production. Worldwide interest in developing specialty coffee has grown; in particular, the high-quality Arabica coffee characterized for its superior organoleptic qualities (Geeraert et al., 2019). In Colombia, coffee production is an important industry; thus, the International Coffee Organization considers this country to be the main soft coffee exporter and in 2019/2020, its production reached a total of 14.1 million of 60 kg bags (ICO, 2022). Additionally, Colombian coffee has excellent sensorial attributes, such as its aroma and body (Özdestan et al., 2013). "Specialty coffee" mainly refers to a coffee which possesses desirable, excellent, unique flavor qualities and is of a specific geographical region (Velásquez et al., 2019). The increase in specialty coffee consumption and demand creates an opportunity for producer countries to obtain higher prices in specialized markets (Tolessa et al., 2016).

In order to better preserve the specialty coffee cup quality, the control of the roasting and subsequent storage plays a key role due to the fact that roasting induces the production and/or degradation of several chemical compounds, such as acids, caffeine, lipids and carbohydrates (Barbosa et al., 2019), which also evolve differently depending on storage conditions. Generally, roasted coffee is a highly hygroscopic matrix, readily adsorbing water when interacting with its environment during storage (Iaccheri et al., 2015). Hygroscopicity may affect coffee freshness, modifying its desirable sensory attributes and affecting the expected value for this differentiated product in international commerce. The storage conditions, temperature and relative humidity, and the state of the coffee (bean or ground) could play a major role in the water absorption process due to the fact that these parameters are indispensable in the food-surrounding medium interactions (Tripetch & Borompichaichartkul, 2019). Thus, adsorption isotherms are a highly

* Corresponding author.
E-mail addresses: gentil.collazos@usco.edu.co (G.A. Collazos-Escobar), ngutierrezg@usco.edu.co (N. Gutiérrez-Guzmán), havaquiro@ut.edu.co (H.A. Váquiro-Herrera), jbon@tal.upv.es (J. Bon), jogarpe4@tal.upv.es (J.V. Garcia-Perez).

https://doi.org/10.1016/j.lwt.2022.113335
Received 27 April 2021; Received in revised form 31 January 2022; Accepted 7 March 2022
Available online 9 March 2022

suitable means of interpreting the water sorption mechanism and interactions between water and foodstuff components and for computing relevant parameters, such as shelf-life and critical moisture level; they are also reliable criteria for the selection of packaging material (Arslan-Tontul, 2020).

According to Anastopoulos et al. (2017) the water adsorption process occurring on a food's solid surface depends on several factors, such as the physicochemical properties, the chemical characteristics of adsorbates, the prevailing experimental conditions, and the affinity between adsorbent-absorbate. The ATR−FTIR spectroscopy technique can be applied as a way of detecting the functional groups available on the adsorption surface of the food material and their effect on the water sorption capacity (Rojas et al., 2020). To our knowledge, different studies have previously used this technique to analyze the sorption behavior of many dehydrated food products, such as dried and roasted cocoa beans (Collazos-Escobar, Gutiérrez-Guzmán, et al., 2020) and dried specialty parchment coffee beans (Collazos-Escobar, Gutierrez Guzman, et al., 2020). These previous studies have reported the ability of this technique to aid understanding of the mechanisms of water sorption in food products similar to roasted coffee.

The use of dynamic dewpoint instruments (DDI) for the experimental assessment of adsorption isotherms offers several advantages over the standard gravimetric method (Mutlu et al., 2020). Specifically, DDI report a better resolution and high-speed analysis (Yao et al., 2020) and a larger number of experimental data (Fan et al., 2017) at considerably lower cost. These aspects are essential for the further modeling of water adsorption isotherms in order to predict the equilibrium moisture content at different water activity levels and temperatures (Aouaini et al., 2015). DDI has been used for the analysis of the moisture adsorption of coffee in different processing stages: coffee cherry beans (Velásquez et al., 2021) and green and roasted coffee beans (Iaccheri et al., 2015). Previous studies evidenced the reliability of DDI analysis, which provided a similar relationship between the water activity-equilibrium moisture content to the gravimetric method. However, in previous studies, there exists a lack of understanding as regards the effect of the temperature on the adsorption process and its quantification based on computer modeling, and nor has the comparison between the behavior of whole and ground beans been sufficiently studied. These aspects are essential for optimizing the storage and transportation conditions and improving cup quality.

Due to the highly complex nature of food, there is not one unique model with which to represent the adsorption isotherms of all agricultural products (Bon et al., 2012). Therefore, it is highly convenient to test the ability of different models to describe the adsorption isotherms when addressing a new analysis of a food commodity. Computer modeling has already been applied in the analysis of the moisture adsorption of green and roasted coffee beans (Iaccheri et al., 2019); roasted ground coffee (Mutlu et al., 2020), and the desorption of coffee cherry beans (Velásquez et al., 2021). These authors claimed the ability of the Guggenheim-Anderson-de Boer (GAB) equation to represent the hygroscopic capacity of coffee in different processing stages. Additionally, empirical models (Peleg, Smith, Oswin) also have adequate capacity to model the adsorption isotherms of both coffee (Mutlu et al., 2020) and different agricultural products (Yogendrarajah et al., 2015). Nevertheless, to our knowledge, robust computer modeling using a large number of experimental data and taking the effect of temperature into consideration has not been employed in the case of roasted ground coffee; this constitutes a powerful tool with which to predict the water adsorption behavior of the product in order to guarantee cup quality.

From accurate experimental adsorption isotherms and robust mathematical models, thermodynamic properties (Gibbs free energy, differential enthalpy, and entropy) can also be computed. Thermodynamic properties are essential for the understanding of the stability of dehydrated food products during storage and their shelf-life (Velázquez--Gutiérrez et al., 2015). Consequently, the thermodynamic analysis of sorption data provides a reliable perspective into the interaction between water molecules and the solid matrix. Differential thermodynamic properties have previously been studied in coffee fruits, and pulped and green coffee beans by Goneli et al. (2013) and roasted coffee by de Oliveira et al. (2016). Nonetheless, these properties have not been quantified in roasted specialty coffee; thus, their knowledge supplies trustworthy information for industrial applications in order to optimize the storage conditions for minimizing the degradation of coffee quality.

If the aforementioned aspects are considered, the main aims of this study are: (i) to experimentally determine the water vapor adsorption isotherms of roasted coffee beans and ground roasted coffee at temperatures of 25, 35 and 45 °C and water activities of between 0.1 and 0.9 using the DDI method; (ii) to address the computer modeling of the adsorption isotherms so as to describe the influence of the water activity and temperature on the equilibrium moisture content and (iii) to assess the hygroscopic capacity of roasted coffee through differential thermodynamic analysis.

2. Materials and methods

2.1. Coffee processing

Nine coffee samples (10 kg), variety (*Coffee arabica* L. cv. Colombia), from different growing areas in the Huila region of Colombia, were processed by the wet method (Velásquez et al., 2019). Each coffee bean sample was pulped (Gaviota 300, Ingesec, Colombia) and fermented in plastic containers for 18 h (Velásquez et al., 2019). The fermented beans were washed and sun-dried until reaching a moisture content of 10–12 (% w.b.). The moisture evolution during drying was monitored with a handheld portable grain moisture tester (Kett PM−450, Science of Sensing, Japan). The sun-drying process was conducted between 9 a.m. and 4 p.m. daily and the room conditions were 37 ± 3 °C and 25–45% R. H. Sensory analysis was carried out on the samples following the Specialty Coffee Association methodology (SCA, 2020), in the Centro Surcolombiano de Investigación en Café (CESURCAFÉ) by five highly trained coffee-sensory panelists (Di Donfrancesco et al., 2014) and classified as specialty coffee. The origin and cup quality score of coffee samples are shown in Table 1.

2.1.1. Roasting and grinding conditions

Prior to roasting, the beans were hulled in a laboratory hulling machine (ING-C-250, Ingesec, Colombia). For each sample, 150 g of healthy green coffee beans were roasted using laboratory rotatory equipment (TC-150R, Quantik, Colombia), which allows an accurate control of time and temperature. The roasting program consisted of the preheating of the rotatory system at 150 °C for 10 min, heating until 185 ± 2 °C and, finally, cooling to 178 ± 2 °C and then the samples were loaded into the roasting chamber. During roasting, the temperature was monitored at time intervals of 5 s. After 3.5 min of roasting, the heating power level was increased from 10 to 60% and roasting finished when the total process time and final temperature were 9 ± 0.5 min and 183 ± 2 °C, respectively. This roasting process, with a luminosity (L*) coordinate value of between 18 and 25 (Craig et al., 2018), could be considered to be medium intensity. To verify this roasting level, the

Table 1
Coffee sample characteristics and sensory classification.

Sample	Origin	Cup score	Classification
1	Cerro Neiva	86	Specialty coffee
2	Cerro Neiva	88	Specialty coffee
3	Tello	85.75	Specialty coffee
4	Colombia	84.5	Specialty coffee
5	Santa María	84	Specialty coffee
6	Palermo	84	Specialty coffee
7	Palermo	84.75	Specialty coffee
8	San Agustín	84.5	Specialty coffee
9	San Agustín	86.5	Specialty coffee

spectrocolorimeter (CR−410, Konica Minolta, N.J. USA) was used considering standard light source D65 and standard observer 10°. Previously, the instrument calibration was performed with a standard white plate (Y = 87.0, x = 0.3160, y = 0.3231). The roasted coffee beans were independently ground in a milling device (Bunn G3 HD-Coffee Mill, Springfield, IL. USA) and separated into medium (particles retained in a #20 standard sieve with a hole diameter of 850 μm) and fine-sized particles (particles retained in a #30 standard sieve with a hole diameter of 600 μm). The samples were classified in a vibratory sieve shaker (EFL-2000, Endecotts LTD, London, U.K) for 10 min.

2.2. Initial moisture content and water activity

The moisture content was determined by drying 5.0 g of samples in an oven (UF55, Memmert GmbH + Co.KG, Schwabach, Germany) at 105 ± 1 °C until constant weight (Mutlu et al., 2020). All of the gravimetric determinations were carried out in triplicate and the results were expressed as percentage of dry basis (% d.b.). For water activity (a_w) measurements, a vapor sorption analyzer (VSA Aqualab, Decagon Devices, Inc. Pullman, WA) was used.

2.3. Attenuated total reflectance fourier-transform infrared (ATR−FTIR) spectroscopy

An FTIR Spectrophotometer (Cary 630, Agilent Technologies, USA) coupled with a horizontal ATR sampling accessory (Diamond ATR) equipped with a ZnSe cell was used to obtain the mid-infrared (MIR) information. The ATR−FTIR measurements were taken in a dry atmosphere at a room temperature of 20 ± 0.5 °C (Craig et al., 2018). The roasted coffee beans were ground (BB004NR0IL2, Bezzera, Italy), and separated using a standard sieve with a hole diameter of 250 μm; approximately 1 g of these ground roasted coffee samples was placed in the sampling accessory and pressed. Background measurements were obtained from readings of the accessory without the sample. All of the infrared spectra were obtained in the MIR at a wavenumber of between 4000 and 650 cm^{-1}, using an 8 cm^{-1} resolution, scan rate of 20, and background correction (Collazos-Escobar, Gutiérrez-Guzmán, et al., 2020). All of the samples were analyzed in triplicate. The preprocessing of MIR spectral data was performed using R-statistical software (version 3.6.3, R statistics, St. Louis, MO, USA) on raw signals. Thus, a baseline correction was performed in order to remove the bias linked to the experimental assessment of the spectrum. The spectral correction was performed using the *baselineSpectra* function of *ChemoSpec* R-package (Hanson, 2022).

2.4. Experimental determination of the water vapor adsorption isotherms

The water vapor adsorption isotherms were determined via the dynamic dewpoint isotherm (DDI) method, using a vapor sorption analyzer (VSA Aqualab Decagon Devices, Inc. Pullman, WA). All of the tests were performed in triplicate over a water activity range of 0.1–0.9 with intervals of 0.01 a_w, and at temperatures of 25, 35, and 45 °C, under an air flow of 100 mL min^{-1}. In every test, 3.5 g samples of roasted coffee beans and ground roasted coffee (medium and fine particle sizes) were placed inside the DDI instrument.

2.5. Mathematical modeling and statistical analysis

The water vapor adsorption isotherms of roasted and ground coffee samples were mathematically described using ten different models, which are compiled in Table 2 (Equations 1 to 12). These models were chosen from the ones most frequently used in literature.

The non-linear fitting of the isotherm models to experimental data was performed with MATLAB® R2021a (The MathWorks Inc., Natick, MA, USA). The "Curve Fitting" tool was used to identify the model parameters and calculate the 95% confidence intervals for the non-linear regression analysis. The adjusted coefficient of determination (R^2_{adj}) (Eq. (13)) and the root mean square error (RMSE) (Eq. (14)) were considered in order to evaluate the goodness of fit of the model. According to Sormoli and Langrish (2015), figures of RMSE <10% d.b. and $R^2_{adj} > 0.98$ reflect a reasonably satisfactory fitting.

Table 2
Mathematical models used to describe the water vapor adsorption isotherms of roasted specialty coffee.

Model	Mathematical expression		Eq. No
GAB	$X_e = \frac{X_m \ CKa_w}{(1-Ka_w)(1+(C-1)Ka_w)}$ $C = C_0 \ \exp\left(\frac{H_m - H_n}{RT}\right)$ $K = K_0 \ \exp\left(\frac{L_r - H_n}{RT}\right)$	García-Pérez et al. (2008)	1 2 3
Iglesias and Chirife	$X_e = b_1 + b_2\left(\frac{a_w}{1-a_w}\right)$	Arslan-Tontul (2020)	4
Halsey	$X_e = \left(\frac{-b_1}{\ln a_w}\right)^{1/b_2}$	(Fan et al., 2019)	5
Smith	$X_e = b_1 - b_2 \ln(1-a_w)$	Arslan-Tontul (2020)	6
Oswin	$X_e = b_1\left(\frac{a_w}{1-a_w}\right)^{b_2}$	Domian et al. (2018)	7
Henderson	$X_e = \left[\frac{-\ln(1-a_w)}{b_1}\right]^{1/b_2}$	(Fan, Zhang, & Bhandari, 2019)	8
Peleg	$X_e = b_0 a_w^{b_1} + b_2 a_w^{b_3}$	Arslan-Tontul (2020)	9
Kuhn	$X_e = \left(\frac{b_1}{\ln a_w} + b_2\right)$	Domian et al. (2018)	10
White and Eyring	$X_e = \frac{1}{(b_1 + b_2 a_w)}$	Arslan-Tontul (2020)	11
DLP	$X_e = b_0 + b_1 x + b_2 x^2 + b_3 x^3$ $x = \ln(-\ln a_w)$	Yogendrarajah et al. (2015)	12

Where X_e is the equilibrium moisture content (% d.b.), a_w is the water activity, X_m is the monolayer equilibrium moisture content (% d.b.), K, K_0, C and C_0 are the Guggenheim-Anderson-de Boer (GAB) model parameters, H_m and H_n are the water sorption heats of the monolayer and multilayer (kJ mol^{-1}), respectively, L_r is the latent heat of vaporization of pure water (kJ mol^{-1}), T is the absolute temperature (K). Meanwhile, the b_i terms represent the parameters for the empirical models in which the temperature dependence was assumed to be linear according to Collazos-Escobar, Gutiérrez-Guzmán, et al. (2020).

$$R^2_{adj} = 1 - \left(\frac{N-1}{N-M}\right)(1-R^2) \quad (13)$$

$$RMSE = \sqrt{\frac{1}{N}\sum_{i=1}^{N}\left(X_{exp} - X_{pred}\right)^2} \quad (14)$$

where X_{exp} and X_{pred} are the experimental and predicted equilibrium moisture contents (% d.b.), respectively. N is the number of experimental data points; M is the number of estimated model parameters and R^2 is the coefficient of determination between the experimental and predicted values.

2.6. Adsorption surface area

The adsorption surface area, S_A (m^2 g^{-1} dry basis), of roasted coffee beans and ground roasted coffee was calculated by means of Eq. (15), according to Tao et al. (2018), using the monolayer moisture content from the linearized BET model (Eq. (16)) evaluated at 25 °C.

$$S_A = X_{mBET}\left(\frac{1}{M_w}\right)N_0 A_W \quad (15)$$

$$\frac{a_w}{(1-a_w)X_e}=\frac{1}{X_{mBET}C_{BET}}+\frac{C_{BET}-1}{X_{mBET}C_{BET}}a_w \quad (16)$$

where, X_{mBET} is the monolayer equilibrium moisture content (% d.b.), M_w is the molecular weight of water (kg mol^{-1}), N_0 is the Avogadro number (6×10^{23} molecules mol^{-1}), A_W is the area for a water molecule (1.06×10^{-19} m^2 molecule^{-1}), and C_{BET} is the BET model parameter.

2.7. Thermodynamic analysis

The hygroscopic capacity of roasted specialty coffee was computed by differential thermodynamic analysis. Thereby, and as explained below, the net isosteric heat, Gibbs free energy and entropy of adsorption were computed from the water vapor adsorption isotherms experimentally obtained at different temperatures using a differential strategy.

2.7.1. Determination of the net isosteric heat of adsorption

The net isosteric heat of adsorption, or enthalpy of adsorption (q_{st}), was calculated using the Clausius-Clapeyron equation (Eq. (17)). The graphical method was used to assess the net isosteric heat of adsorption for a specific moisture content, wherein the slope and y-intercept obtained of the linear fitting between ln (a_w) and 1/T at a constant equilibrium moisture content was employed (Červenka et al., 2019).

$$q_{st}=-R\left[\frac{\partial(\ln a_w)}{\partial\left(\frac{1}{T}\right)}\right]_{X_e} \quad (17)$$

where, a_w is water activity, R is the universal gas constant of water vapor (8.314×10^{-3} kJ mol^{-1} K^{-1}), T is the absolute temperature (K) and X_e is the equilibrium moisture content (% d.b.).

2.7.2. Determination of gibbs free energy and adsorption entropy

The Gibbs free energy (ΔG) is linked to the spontaneous nature of the water vapor sorption process, which was computed from Eq. (18).

$$\Delta G = RT \ \ln \ (a_w) \quad (18)$$

The change in the differential adsorption entropy (ΔS_d) can be calculated from Eq. (19).

$$\Delta S_d=\frac{q_{st}-\Delta G}{T} \quad (19)$$

3. Results and discussion

3.1. Experimental water vapor adsorption isotherms

The water vapor adsorption isotherms of roasted and ground specialty coffee samples are shown in Fig. 1. The isotherms show a J-Curve shape characteristic of type III curves, according to the Brunauer-Emmett-Teller (BET) classification, which is typical of mainly crystalline matrices and representative of food products rich in soluble components, such as sugars (Herman et al., 2018). Similar adsorption isotherms were also obtained by Iaccheri et al. (2019) studying green and roasted coffee beans, Yogendrarajah et al. (2015) working on whole black peppercorns, and Collazos-Escobar, Gutiérrez-Guzmán, et al. (2020) analyzing dried and roasted cocoa beans. This sorption shape can be explained by the chemical transformation that the coffee undergoes during the roasting process linked to the Maillard reaction and the caramelization of sugars (García-Alamilla et al., 2017).

According to Domian et al. (2018), the reduction in the amount of water adsorbed when the temperature increases at constant water activity is widely accepted. In this sense, foodstuffs adsorb more water at low temperatures, which indicates that the water molecules have more kinetic energy at high temperatures, and which is enough to overcome

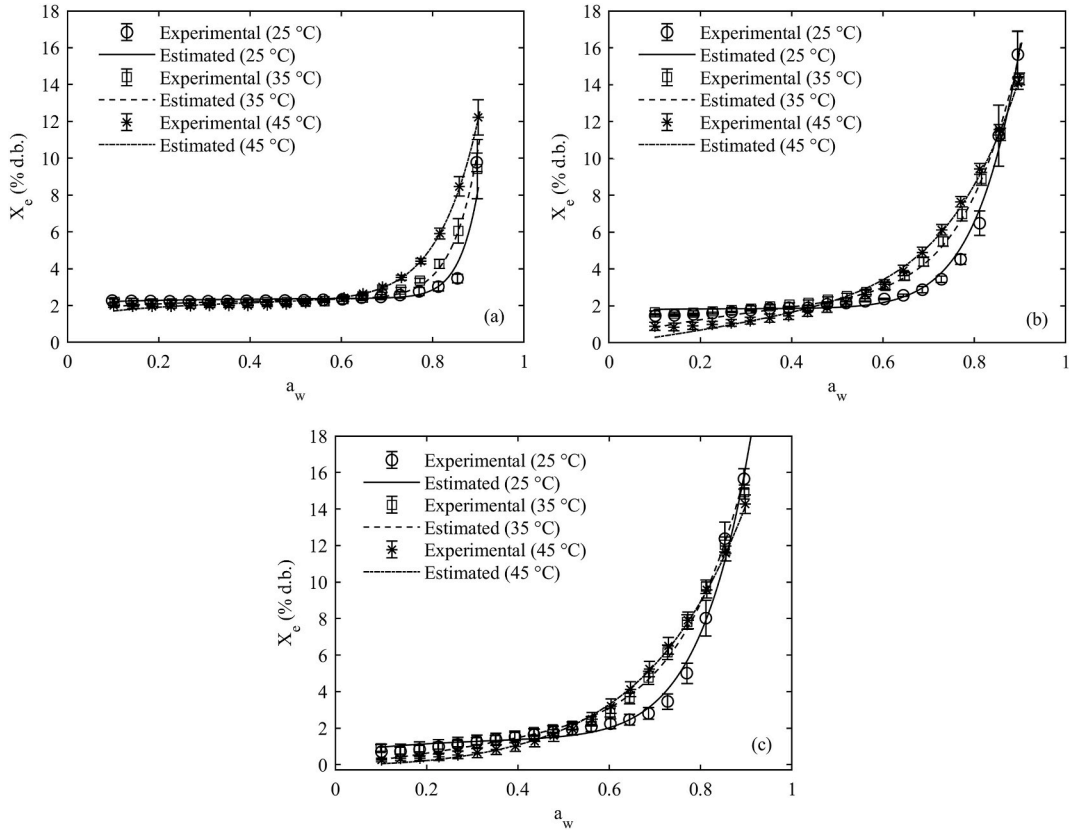

Fig. 1. Experimental water vapor adsorption isotherms and Peleg model fitting for roasted coffee beans (a) and medium (b) and fine (c) ground roasted coffee at 25, 35, and 45 °C.

the energy linked to the sorption site. Therefore, the food product becomes less hygroscopic as a result of the temperature increase. As illustrated in Fig. 1b and c, at low water activity (0.1–0.52 a_w), the influence of the temperature on the isotherms for ground coffee follows the typical behavior mentioned above, but the effect is not significant ($p > 0.05$). In the case of whole coffee beans (Fig. 1a), however, isotherms at different temperatures completely overlap at low water activities (0.1–0.6 a_w for coffee beans).

As water adsorption progressed, the expected effect of the temperature was not found at high water activities (a_w>0.6 for roasted coffee beans and a_w>0.52 for ground coffee), and the isotherms reflected an inverse phenomenon. Thus, the rise in temperature at constant water activity led to a higher equilibrium moisture content, and consequently, greater water availability. This led to the crossing of the isotherms-curves at the different temperatures, as observed in Fig. 1b and c. These results can be explained in terms of the solubilization of the sugars contained in the food matrix at high temperatures and water activities. Indeed, at high water activities, the water molecules can be available as a solvent of low molecular weight solutes (Domian et al., 2018). The inverse effect of the temperature has been reported in several food and agricultural products: whole black peppercorns (Yogendrarajah et al., 2015), green and roasted yerba mate (Červenka et al., 2015), starch albumen powder (Shittu et al., 2015), spray-dried fat-filled pea protein-based powders (Domian et al., 2018), borojó fruit and gum arabic powders (Rodríguez-Bernal et al., 2015), and roasted cocoa beans (Collazos-Escobar, Gutiérrez-Guzmán, et al., 2020). Therefore, the dissolution of the sugars at high water activities and the adsorbate-adsorbent interactions could affect the typical adsorption mechanism.

As for the role of the bean structure and its influence on the hygroscopic capacity of specialty roasted coffee, Fig. 1a shows an asymptotical evolution of the equilibrium moisture content of roasted coffee beans in water activities of between 0.1 and 0.6. In this water activity region, the equilibrium moisture content remains almost constant regardless of the water activity, showing that the bean structure does not change the amount of adsorbed water when exposed to different environments, behaving differently from what may be observed in the case of the ground material. This result can be explained by the increase in the adsorption surface area as the particles become smaller in the ground product. Likewise, slight differences can also be found between the concave upward J-shape type III isotherms of roasted and ground-roasted coffee beans, as illustrated in Fig. 1. These results are of interest as they help to explain the hygroscopic behavior of roasted coffee, which will be discussed in section 3.5.

3.2. Computed modeling of water adsorption isotherms

Tables 3–5 show the results of modeling water isotherms considering the effect of temperature on the water vapor adsorption isotherms of roasted and ground specialty coffee. As already explained, the criteria to select the best model were the lowest error (RMSE) and the highest R^2_{adj}. In this sense, the modeling results reported that the Peleg model provided a satisfactory description of the adsorption behavior of roasted coffee beans ($R^2_{adj} = 0.96$ and RMSE = 0.49% d.b.) and ground-roasted coffee of medium ($R^2_{adj} = 0.98$ and RMSE = 0.53% d.b.) and fine particle sizes ($R^2_{adj} = 0.99$ and RMSE = 0.44% d.b.). The goodness of fit of the Peleg model is illustrated in Fig. 1 in which the modeling and experimental results are plotted together. The fitting-ability of the Peleg equation has been successfully evidenced both in roasted and ground coffee beans (Mutlu et al., 2020), and in other agricultural products, such as whole black peppercorns (Yogendrarajah et al., 2015) and in microencapsulated extra virgin olive oil (Bastıoğlu et al., 2017).

In the case of the remaining empirical equations, and for practical purposes, the DLP model for roasted coffee beans could also be considered for the mathematical representation of the adsorption isotherms due to its adequate fitting capacity, as could the Iglesias & Chirife, Oswin, Kuhn, White & Eiring and the DLP for ground-roasted coffee of medium and fine particle sizes. However, the statistics of the other three models (Smith, Henderson, and Halsey) did not reflect a close agreement between experimental and estimated adsorption data and should not be chosen to represent the hygroscopic behavior of specialty coffee.

Table 3
Estimated model parameters and statistical results of roasted coffee beans.

Model	Parameters	Confidence Intervals 95%	R^2_{adj}	RMSE (% d.b.)
GAB	$X_m = 0.85\%$ d.b. $C_0 = 101$ $K_0 = 433$ $H_m = 198.6$ kJ mol^{-1} $H_n = 59.1$ kJ mol^{-1}	[0.82, 0.88] [-1.886×10^8, 1.886×10^8] [390, 477] [-356.8×10^6, 356.8×10^6] [58.8, 59.4]	0.89	0.77
Iglesias & Chirife	$b_{2.1} = -7.6$ $b_2 = 0.028$ K^{-1} $b_{1.1} = 7$ $b_1 = -0.02$ K^{-1}	[−8.6, −6.6] [0.024, 0.03] [3, 11] [-0.03, -6.23×10^{-3}]	0.89	0.76
Oswin	$b_{2.1} = -2$ $b_2 = 9.15 \times 10^{-3}$ K^{-1} $b_1 = 5.09 \times 10^{-3}$ K^{-1}	[−2.31, −1.67] [8.11×10^{-3}, 0.01] [4.66×10^{-3}, 5.53×10^{-3}]	0.85	0.88
Peleg	$b_{3.1} = -1.4$ $b_3 = 4.85 \times 10^{-3}$ K^{-1} $b_{2.1} = 2.45$ $b_{1.1} = 198$ $b_1 = -0.6$ K^{-1} $b_{0.1} = 545$ $b_0 = -1.62$ K^{-1}	[−2.7, −0.1] [7.83×10^{-4}, 8.92×10^{-3}] [2.34, 2.57] [174, 222] [−0.7, −0.5] [381, 710] [−2.14, −1.11]	0.96	0.49
Kuhn	$b_{2.1} = 10.2$ $b_2 = -0.032$ K^{-1} $b_{1.1} = 7.5$ $b_1 = -0.027$ K^{-1}	[5.6, 14.8] [−0.046, −0.017] [6.5, 8.5] [−0.03, −0.024]	0.89	0.77
White & Eiring	$b_{2.1} = -9.6$ $b_2 = 0.027$ K^{-1} $b_{1.1} = 9.5$ $b_1 = -0.03$ K^{-1}	[−11.8, −7.4] [0.02, 0.03] [7.6, 11.4] [−0.03, −0.02]	0.90	0.72
DLP	$b_{3.1} = -9.2$ $b_3 = 0.027$ K^{-1} $b_{2.1} = -31.6$ $b_2 = 0.101$ K^{-1} $b_{1.1} = 6.68$ $b_1 = -0.02$ K^{-1} $b_{0.1} = 17.1$ $b_0 = -0.05$ K^{-1}	[−12.5, −5.9] [0.016, 0.037] [−39.7, −23.5] [0.075, 0.013] [1.24, 12.11] [-0.04, -3.06×10^{-3}] [12.8, 21.3] [−0.06, −0.03]	0.95	0.54

The generalized GAB model did not fit the water vapor adsorption isotherms for roasted specialty coffee well (Tables 3–5). Thus, the GAB model provided a low $R^2_{adj} < 0.95$ and a RMSE of nearly 1% d.b, which can be considered as poor fitting parameters compared to the Peleg equation. However, the GAB model also provided an estimation of the monolayer moisture content (X_m parameter), which can be considered as useful for the purposes of defining an adequate moisture content which ensures stability during the storage of dehydrated food products (Yogendrarajah et al., 2015). Thus, X_m were 0.85% d.b. for roasted coffee beans, 1.27% d.b. and 1.28% d.b. for ground roasted coffee of medium and fine particle sizes, respectively, indicating that the smaller the particle size, the higher the X_m values. This agrees with the results obtained by Mutlu et al. (2020), working on roasted coffee beans and ground coffee, who attributed this trend to the increasing moisture adsorption surface area caused by the grinding process.

3.3. ATR–FTIR analysis

Fig. 2 shows the roasted coffee ATR–FTIR spectra on MIR with baseline correction; the same spectral behavior was observed in all of the

Table 4
Estimated model parameters and statistical results of ground roasted coffee of medium particle size.

Model	Parameters	Confidence Intervals 95%	R^2_{adj}	RMSE (% d.b.)
GAB	$X_m = 1.27\%$ d.b. $C_0 = 114.8$ $K_0 = 188.2$ $H_m = 301.4$ kJ mol^{-1} $H_n = 56.9$ kJ mol^{-1}	[1.23, 1.3] [-1.7×10^8, 1.7×10^8] [174.8, 201.6] [-416.8×10^6, 416.6×10^6] [56.7, 57.1]	0.94	0.92
Iglesias & Chirife	$b_2 = 5.62 \times 10^{-3}$ K^{-1} $b_{1.1} = -6.1$ $b_1 = 0.02$ K^{-1}	[5.52×10^{-4}, 5.72×10^{-3}] [−8.4, −3.7] [0.01, 0.03]	0.95	0.80
Oswin	$b_{2.1} = 3.3$ $b_2 = -7.68 \times 10^{-3}$ K^{-1} $b_{1.1} = -15.8$ $b_1 = 0.06$ K^{-1}	[2.8, 3.8] [-9.35×10^{-3}, -6.02×10^{-3}] [−19.1, −12.5] [0.05, 0.07]	0.95	0.80
Peleg	$b_{3.1} = -17.8$ $b_3 = 0.06$ K^{-1} $b_{2.1} = -42$ $b_2 = 0.15$ K^{-1} $b_{1.1} = 56.7$ $b_1 = -0.16$ K^{-1} $b_{0.1} = 317$ $b_0 = -0.94$ K^{-1}	[−20.9, −14.8] [0.05, 0.07] [−53, −32] [0.11, 0.18] [47.3, 66] [−0.19, −0.13] [282, 352] [−1.1, −0.82]	0.98	0.53
Kuhn	$b_{2.1} = -5.95$ $b_2 = 0.019$ K^{-1} $b_1 = -5.55 \times 10^{-3}$ K^{-1}	[−8.33, −3.58] [0.011, 0.027] [-5.64×10^{-3}, -5.45×10^{-3}]	0.95	0.82
White & Eiring	$b_{2.1} = -5.48$ $b_2 = 0.015$ K^{-1} $b_{1.1} = 4.9$ $b_1 = -0.013$ K^{-1}	[−6.29, −4.67] [0.013, 0.018] [4.2, 5.6] [−0.016, −0.011]	0.95	0.82
DLP	$b_{3.1} = -27$ $b_3 = 0.086$ K^{-1} $b_{2.1} = -39$ $b_2 = 0.13$ K^{-1} $b_{1.1} = 30$ $b_1 = -0.1$ K^{-1} $b_{0.1} = 14$ $b_0 = -0.04$ K^{-1}	[−30, −24] [0.076, 0.096] [−46, −32] [0.11, 0.15] [26, 34] [−0.12, −0.1] [11, 17] [−0.05, −0.03]	0.98	0.55

Table 5
Estimated model parameters and statistical results of ground roasted coffee of fine particle size.

Model	Parameters	Confidence Intervals 95%	R^2_{adj}	RMSE (% d.b.)
GAB	$X_m = 1.28\%$ d.b. $C_0 = 99$ $K_0 = 196$ $H_m = 400$ kJ mol^{-1} $H_n = 57$ kJ mol^{-1}	[1.24, 1.32] [-1.75×10^8, 1.75×10^8] [179, 213] [-727×10^6, 727×10^6] [56.8, 57.2]	0.92	1.1
Iglesias & Chirife	$b_2 = 6.08 \times 10^{-3}$ K^{-1} $b_{1.1} = -3.76$ $b_1 = 0.01$ K^{-1}	[5.98×10^{-3}, 6.17×10^{-3}] [−5.97, −1.54] [5.72×10^{-3}, 0.02]	0.96	0.80
Oswin	$b_{2.1} = 4.03$ $b_2 = -0.01$ K^{-1} $b_{1.1} = -18.62$ $b_1 = 0.07$ K^{-1}	[3.62, 4.45] [−0.01, -8.69×10^{-3}] [−21.18, −16.06] [0.06, 0.08]	0.97	0.73
Peleg	$b_{3.1} = -27.84$ $b_3 = 0.09$ K^{-1} $b_{2.1} = -75.3$ $b_2 = 0.26$ K^{-1} $b_{1.1} = 52$ $b_1 = -0.15$ K^{-1} $b_{0.1} = 335$ $b_0 = -1$ K^{-1}	[−30.42, −25.27] [0.09, 0.1] [−86.2, −64.4] [0.22, 0.3] [46, 58] [−0.17, −0.13] [310, 360] [−1.08, −0.92]	0.99	0.44
Kuhn	$b_{2.1} = -3.6$ $b_2 = 0.01$ K^{-1} $b_1 = -6 \times 10^{-3}$ K^{-1}	[−5.9, −1.4] [2.8×10^{-3}, 0.02] [-6.08×10^{-3}, -5.9×10^{-3}]	0.96	0.80
White & Eiring	$b_{2.1} = -3.2$ $b_2 = 7.84 \times 10^{-3}$ K^{-1} $b_{1.1} = 3$ $b_1 = -7.13 \times 10^{-3}$ K^{-1}	[−4.1, −2.3] [4.88×10^{-3}, 0.01] [2.1, 3.9] [-9.74×10^{-3}, -4.53×10^{-3}]	0.92	1.07
DLP	$b_{3.1} = -22$ $b_3 = 0.07$ K^{-1} $b_{2.1} = -28.6$ $b_2 = 0.10$ K^{-1} $b_{1.1} = 26.7$ $b_1 = -0.09$ K^{-1} $b_{0.1} = 9.36$ $b_0 = -0.027$ K^{-1}	[−25, −19] [0.06, 0.08] [−35.3, −21.9] [0.08, 0.12] [22.6, 30.8] [−0.11, −0.08] [6.79, 11.92] [−0.035, −0.019]	0.98	0.58

roasted coffee samples, due to the fact that the physical structure (coffee beans and ground material) did not affect the chemical molecules. As is illustrated in Fig. 2, the majority of the infrared signals exhibited broadband between 3260 and 1017 cm^{-1}, which included two different spectral regions (i) functional group (3650–1500 cm^{-1}) and (ii) fingerprint (1500–650 cm^{-1}). In order to describe the results obtained, the previous studies must be considered; in this sense, Durak and Depciuch (2020) have reported the chemical compounds and functional groups associated with different mid-infrared ranges:

- 3290–3270 cm^{-1} can be associated with water and polysaccharides
- 2950–2910 cm^{-1}, 2870–2840 cm^{-1}, 1800–1765 cm^{-1}, 1750–1700 cm^{-1} and 1380–1300 cm^{-1} with lipids
- 1650–1620 cm^{-1} with water and proteins
- 1600–1545 cm^{-1} and 1460–1430 cm^{-1} with proteins and lipids
- 1260–1235 cm^{-1} with polysaccharides
- 1160–1145 cm^{-1} and 1120–1100 cm^{-1} with esters
- 1080–1015 cm^{-1} with glycosides
- 840–810 cm^{-1} with aromatic rings
- 770–700 cm^{-1} with C–H rocking.

Based on the Durak and Depciuch (2020) study, the ATR–FTIR spectra of roasted coffee showed a typical vibration pattern of foodstuff constituents, such as proteins, lipids, and carbohydrates, reflecting the major composition of roasted specialty coffee. It can be seen in Fig. 2 that spectral signals exhibited intensities at the wavenumbers mentioned above and were quite similar to the spectrum of roasted coffee reported by Craig et al. (2018), who stated that the relatively high absorbance intensities of arabica coffees at wavenumbers of 2922 cm^{-1}, 2852 cm^{-1}, and 1743 cm^{-1} are mostly associated with lipid absorption, the band at 1153 cm^{-1} is linked to the polysaccharides and 1643 cm^{-1} is usually associated with C═O stretching vibration in caffeine. Additionally, Meza et al. (2018) mentioned that the presence of fats in foodstuffs will influence the water adsorption capacity, due to their hydrophobic or non-polar nature and fat mimetics are normally polar water-soluble compounds that can facilitate water-binding, altering the hygroscopicity and water adsorption properties. With respect to carbohydrates, the increases in hygroscopic capacity are likely caused by sugar dissolution at high water activities and temperatures, resulting in the complete leaching of the sugar, a change in the crystalline structure of the sugar to the amorphous state, and an increase in the number of adsorption sites due to the swelling of the biopolymer (Eim et al., 2011). Consequently, the inverse-phenomenon of water vapor adsorption isotherms at high water activities (Fig. 1) could be explained by the solubility of carbohydrates and the adsorption affinity of water with the lipids found in roasted coffee.

3.4. Adsorption surface area

The specific surface area of adsorption, S_A, for roasted coffee was

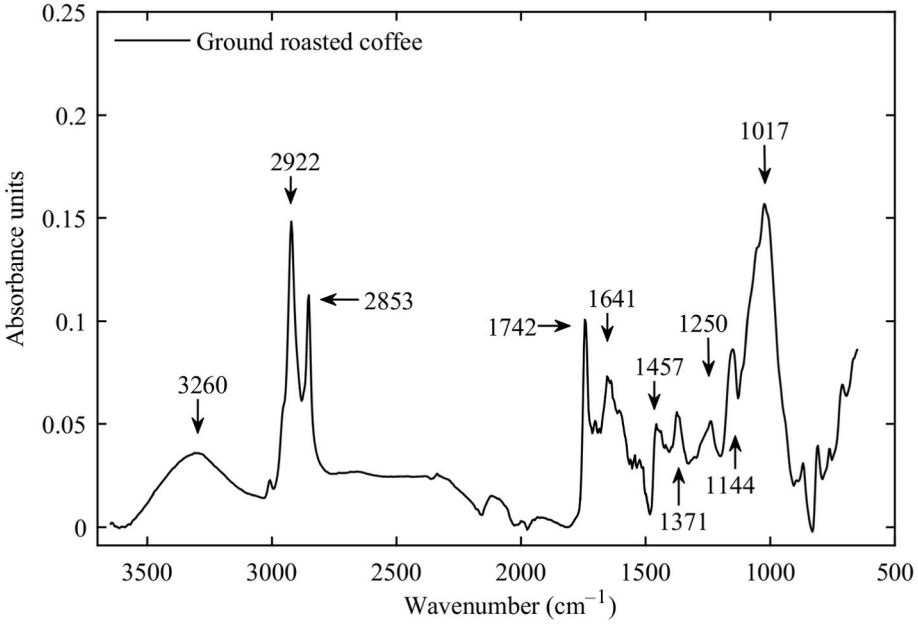

Fig. 2. Average ATR–FTIR spectra of ground roasted coffee.

calculated using the monolayer equilibrium moisture content from the linearized BET model (Eq. (16)) for water activities between 0.1 and 0.6 for roasted coffee beans and 0.1–0.52 for ground coffee, where the usual sorption behavior was found. Similarly to the X_m values obtained by the generalized GAB model (Tables 3–5), the X_{mBET} values at 25 °C were 0.81, 1.04, and 1.16 (% d.b.) for roasted coffee beans and ground roasted coffee of medium and fine particle sizes, respectively, which corresponded to adsorption surface areas of 28.5, 36.8, and 40.9 ($m^2\ g^{-1}$ dry matter). Therefore, the adsorption surface area increased as the particles became smaller. The figures obtained were similar to those reported for roasted coffee beans and ground coffee at 25 °C by Mutlu et al. (2020), who mentioned that the ground coffee samples could bind more water molecules than roasted coffee beans, due to the fact that the ground material contains more active adsorption sites, such as the hydroxyl group. Additionally, when analyzing blueberry powders, Tao et al. (2018) mentioned that the increase in water holding capacity could be ascribed to the decrease in particle size and the increase in surface area.

3.5. Differential thermodynamic analysis

The variations in the net isosteric heat of adsorption and differential adsorption entropy of the roasted and ground roasted coffee beans of different particle sizes are shown in Fig. 3. What can be observed is the decrease in q_{st} that occurs in line with the increase in the equilibrium moisture content for roasted coffee at low moisture contents, between 1.1% and 2% d.b (Fig. 3a), reflecting a normal sorption trend. This result can be explained by considering that at low equilibrium moisture contents, the active sorption sites at the surface can tightly bond the water molecules forming a mono-molecular layer. As adsorption progresses, once these high energy sites have already been occupied, lower energy sites appear (Červenka et al., 2019). Similar results have been reported for different foodstuffs and agricultural products: green and roasted yerba mate (Červenka et al., 2015), roasted and unroasted carob (Červenka et al., 2019), dried and roasted cocoa beans (Collazos-Escobar, Gutiérrez-Guzmán, et al., 2020), whole chia seeds (Arslan-Tontul., 2020), whole black peppercorns (Yogendrarajah et al., 2015), and blueberry powders (Tao et al., 2018). Additionally, as can be observed from moisture contents of over 2%, the water adsorption leads to an

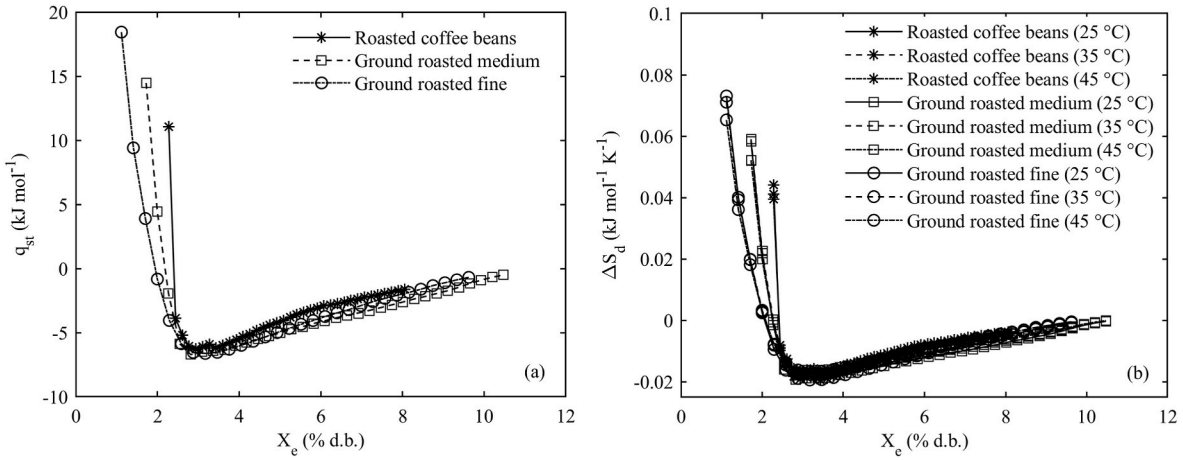

Fig. 3. Net isosteric heat of adsorption (a) and differential adsorption entropy (b) at 25, 35, and 45 °C of beans and medium and fine ground roasted coffee as a function of the equilibrium moisture content.

increase in q_{st}, indicating an inverse effect in the normal thermodynamic behavior.

The negative values of q_{st} can be explained by the inverse temperature effect on the vapor adsorption isotherms at high water activities, as previously shown in Fig. 1. The tendencies observed were similar to those reported in roasted cocoa beans (Collazos-Escobar, Gutiérrez-Guzmán, et al., 2020) and spray-dried fat-filled pea protein-based powder (Domian et al., 2018). The inverse effect of the temperature was also previously ascribed to solute dissolution at high water activities. The functional groups associated with the water-soluble components identified by ATR−FTIR spectroscopy on the roasted specialty coffee samples (Fig. 2) are responsible for the inverse trend of water adsorption properties.

Fig. 3b shows the differential adsorption entropy (ΔS_d) variations at different temperatures. The ΔS_d decreased as the moisture content increased and the temperature influence was not significant ($p > 0.05$). In the moisture content range from 1.1% to 2% d.b. (Fig. 3b), the differences between the ΔS_d of coffee beans and ground roasted coffee was evident. According to Yogendrarajah et al. (2015), sorption entropy can be considered as proportional to the number of available sorption sites at a specific energy level. So, the results suggested that the finely-sized particles had a greater number of available sorption sites at a certain energy level than the medium-sized particles and roasted beans. This can be explained by considering the aforementioned adsorption surface area results (see section 3.4). Additionally, negative ΔS_d values were observed in an equilibrium moisture content of over 2% d.b. This can be explained by changes in the water vapor adsorption trend corresponding to the inverse effect of temperature observed in Fig. 1a, b, and 1c. This is consistent with the data reported by Červenka et al. (2015), who mentioned that the changes caused by roasting may promote the dissolution of sugars at high water activities and temperatures causing changes in the sorption properties. The results observed in Fig. 2b were similar to those reported by Collazos-Escobar, Gutiérrez-Guzmán, et al. (2020) when studying roasted and raw cocoa beans, who found the inverse adsorption phenomenon for water activities of over 0.8. Collazos-Escobar, Gutiérrez-Guzmán, et al. (2020) claimed that the modification of the differential thermodynamic properties of the cocoa beans linked to the roasting process could be ascribed to the dissolution of sugars and other water-soluble components. If roasted coffee and cocoa are compared, the a_w point at which the inverse adsorption behavior occurred shifted from 0.5 to 0.6 in coffee to 0.8 in cocoa, suggesting that the specificity of the adsorption inverse-phenomenon is characteristic for each food material.

Fig. 4 shows Gibbs free energy changes as a function of temperature and the equilibrium moisture content of roasted coffee beans and ground roasted coffee of different particle sizes. Gibbs free energy (ΔG) represents the affinity of adsorbing materials to water molecules; the negative values are commonly associated with the spontaneous exothermic process, which does not require an input of energy from the surrounding environment (Cheng et al., 2020). ΔG figures approached zero as the equilibrium moisture content increased for roasted coffee beans and roasted ground coffee of medium and fine particle sizes (Fig. 4), indicating that there are fewer available sorption sites at higher moisture levels (Cano-higuita et al., 2013). Moreover, the negative ΔG values indicated that adsorption in roasted specialty coffee is naturally spontaneous. Gibbs free energy has been reported to behave similarly in roasted coffee (de Oliveira et al., 2016), dried and roasted cocoa beans (Collazos-Escobar et al., 2020), spray-dried mango mix powders (Cano-higuita et al., 2013), and whole black peppercorns (Yogendrarajah et al., 2015).

As mentioned above when dealing with the effect of the bean structure on hygroscopic capacity, this hypothesis can be confirmed through Fig. 4, in which differences between the ΔG values for roasted coffee beans and ground coffee can be observed. As the moisture content

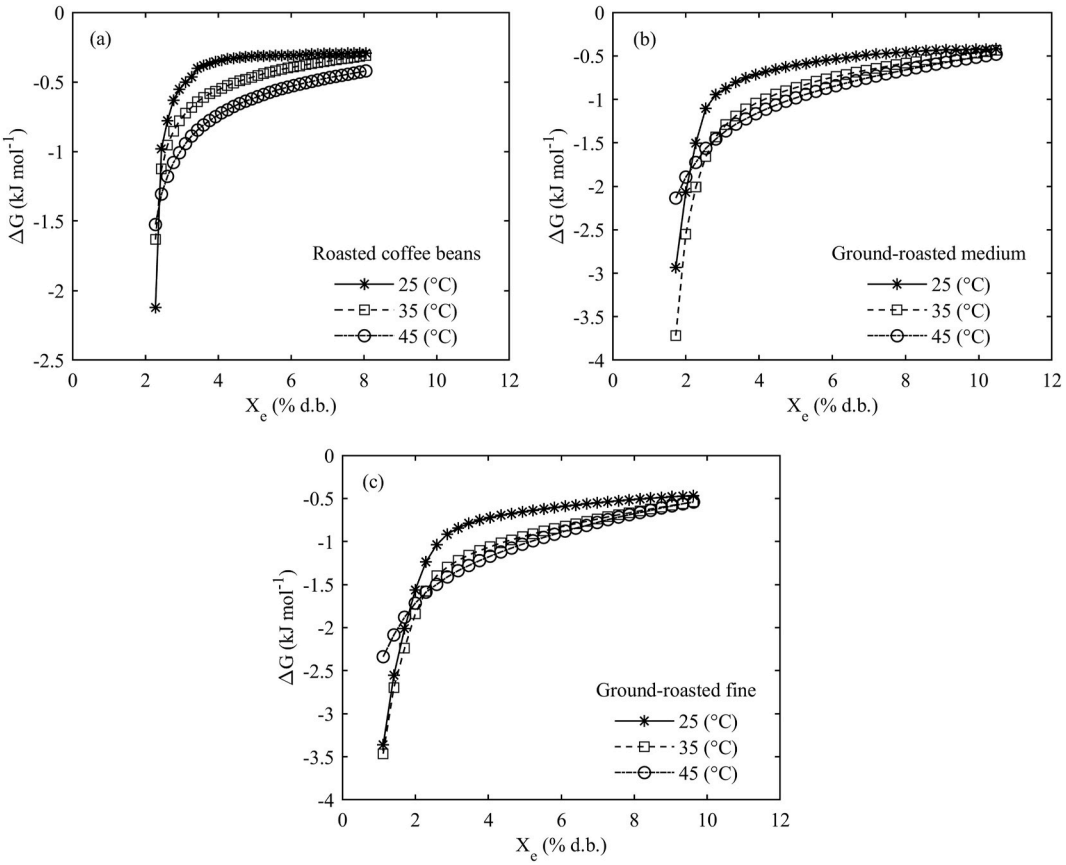

Fig. 4. Gibbs free energy of beans (a) and medium (b) and fine (c) ground roasted coffee at 25, 35, and 45 °C as a function of the equilibrium moisture content.

of the ground material increased, there was a noticeably smaller amount of ΔG (energy released) than in the case of coffee beans. According to the criterion of spontaneity (ΔG<0), lower Gibbs free energy values indicate greater hygroscopicity. Based on this fact, it can be inferred that when roasted coffee beans are ground, the specific surface area of adsorption increases, promoting the binding of more water molecules on a greater number of available adsorption sites (Fig. 3b) with higher energy, as illustrated in Fig. 3a.

4. Conclusions

The water vapor adsorption behavior of roasted and ground roasted coffee beans of medium and fine particle sizes exhibited a type III shape typical of sugar-rich food products. An inverse temperature effect on water vapor adsorption isotherms was manifested at high water activities (from 0.5 to 0.6 to 0.9.); according to the previous results and the FTIR analysis, this should be ascribed to the possible sugar dissolution and the adsorbate-adsorbent interactions in roasted specialty coffee.

The adsorption isotherms were satisfactorily modeled by the Peleg equation, which could be considered as a valuable tool with which to predict and optimize the storage conditions for water activities between 0.1 and 0.9 and at temperatures of 25, 35 and 45 °C. Due to the inverse adsorption phenomenon, the theoretical GAB model was not able to describe the adsorption process adequately.

Ground coffee evidenced a greater differential entropy associated with a larger number of polar available adsorption sites than coffee beans, and also presented a higher net isosteric heat of adsorption, which is explained by a greater spontaneity (Gibbs free energy) during the hydration process.

From the thermodynamic analysis and modeling of the water vapor adsorption isotherms, it was clear that the bean structure offered a more protective role against water vapor adsorption than the ground material. Consequently, the results of this study revealed that coffee should be stored as beans in order to guarantee its stability.

CRediT authorship contribution statement

Gentil A. Collazos-Escobar: Conceptualization, Data curation, Formal analysis, Investigation, Methodology, Software, Supervision, Validation, Visualization, Writing – original draft, Writing – review & editing. **Nelson Gutiérrez-Guzmán:** Conceptualization, Data curation, Formal analysis, Funding acquisition, Investigation, Project administration, Resources, Software, Supervision, Validation, Visualization. **Henry A. Váquiro-Herrera:** Conceptualization, Data curation, Formal analysis, Investigation, Methodology, Supervision, Validation, Visualization. **José Bon:** Data curation, Formal analysis, Software, Validation. **José V. Garcia-Perez:** Conceptualization, Investigation, Software, Validation, Visualization, Writing – original draft, Writing – review & editing.

Declaration of competing interest

None.

Acknowledgments

The authors thank the Centro Surcolombiano de Investigación en Café (CESURCAFÉ) of the Universidad Surcolombiana Neiva-Huila of Colombia and the Grupo de Análisis y Simulación de Procesos Agroalimentarios (ASPA) of the Universitat Politècnica de València-España, for their support which was indispensable for this study.

References

Anastopoulos, I., Karamesouti, M., Mitropoulos, A. C., & Kyzas, G. Z. (2017). A review for coffee adsorbents. *Journal of Molecular Liquids, 229*, 555–565. https://doi.org/10.1016/j.molliq.2016.12.096

Aouaini, F., Knani, S., Yahia, M. B., & Lamine, A. B. (2015). Statistical physics studies of multilayer adsorption isotherm in food materials and pore size distribution. *Physica A, 432*, 373–390. https://doi.org/10.1016/j.physa.2015.03.052

Arslan-Tontul, S. (2020). Moisture sorption isotherm, isosteric heat and adsorption surface area of whole chia seeds. *Lebensmittel-Wissenschaft & Technologie, 119* (October 2019), 108859. https://doi.org/10.1016/j.lwt.2019.108859

Barbosa, M. de S. G., Scholz, M. B., dos, S., Kitzberger, C. S. G., & Benassi, M. de T. (2019). Correlation between the composition of green Arabica coffee beans and the sensory quality of coffee brews. *Food Chemistry, 292*(April), 275–280. https://doi.org/10.1016/j.foodchem.2019.04.072

Bastıoğlu, A. Z., Koç, M., & Kaymak, F. (2017). Moisture sorption isotherm of microencapsulated extra virgin olive oil by spray drying. *Journal of Food Measurement and Characterization*. https://doi.org/10.1007/s11694-017-9507-4

Bon, J., Vaquiro Herrera, H. A., & Mulet, A. (2012). Modeling sorption isotherms and isosteric heat of sorption of mango pulp cv. Tommy atkins. *Biotecnología en el Sector Agropecuario y Agroindustrial, 10*(2), 34–43.

Cano-higuita, D. M., Villa-vélez, H. A., Telis-romero, J., Alexander, H., Regina, V., & Telis, N. (2013). Food and bioproducts processing influence of alternative drying aids on water sorption of spray dried mango mix powders : A thermodynamic approach. *Food and Bioproducts Processing, 93*(June), 19–28. https://doi.org/10.1016/j.fbp.2013.10.005

Červenka, L., Hloušková, L., & Žabčíková, S. (2015). Moisture adsorption isotherms and thermodynamic properties of green and roasted Yerba mate (Ilex paraguariensis). *Food Bioscience, 12*, 122–127. https://doi.org/10.1016/j.fbio.2015.10.001

Červenka, L., Stępień, A., Frühbauerová, M., Velichová, H., & Witczak, M. (2019). Thermodynamic properties and glass transition temperature of roasted and unroasted carob (Ceratonia siliqua L.) powder. *Food Chemistry, 300*(July), 125208. https://doi.org/10.1016/j.foodchem.2019.125208

Cheng, X., Zhang, M., & Adhikari, B. (2020). Moisture adsorption in water caltrop (Trapa bispinosaRoxb.) pericarps: Thermodynamic properties and glass transition. *Journal of Food Process Engineering*. https://doi.org/10.1111/jfpe.13442. *March*, 1–11.

Collazos-Escobar, G. A., Gutierrez Guzman, N., Váquiro-Herrera, H. A., & Amorocho-Cruz, C. M. (2020). Moisture dynamic sorption isotherms and thermodynamic properties of parchment specialty coffee (Coffea arabica L.). *Coffee Science, 15*, 1–10. https://doi.org/10.25186/.v15i.1684, 2020.

Collazos-Escobar, G. A., Gutiérrez-Guzmán, N., Váquiro-Herrera, H. A., & Amorocho-Cruz, C. M. (2020). Water dynamics adsorption properties of dried and roasted cocoa beans (theobroma cacao L.). *International Journal of Food Properties, 23*(1). https://doi.org/10.1080/10942912.2020.1732408

Craig, A. P., Botelho, B. G., Oliveira, L. S., & Franca, A. S. (2018). Mid infrared spectroscopy and chemometrics as tools for the classification of roasted coffees by cup quality. *Food Chemistry, 245*(November), 1052–1061. https://doi.org/10.1016/j.foodchem.2017.11.066

Di Donfrancesco, B., Gutierrez Guzman, N., & Chambers, E. (2014). Comparison of results from cupping and descriptive sensory analysis of colombian brewed coffee. *Journal of Sensory Studies, 29*(4), 301–311. https://doi.org/10.1111/joss.12104

Domian, E., Brynda-kopytowska, A., Cie, J., & Agata, G. (2018). Effect of carbohydrate type on the DVS isotherm-induced phase transitions in spray-dried fat- fi lled pea protein-based powders. *Journal of Food Engineering, 222*, 115–125. https://doi.org/10.1016/j.jfoodeng.2017.11.012

Durak, T., & Depciuch, J. (2020). Effect of plant sample preparation and measuring methods on ATR-FTIR spectra results. *Environmental and Experimental Botany, 169* (October 2019), 103915. https://doi.org/10.1016/j.envexpbot.2019.103915

Eim, V. S., De, U., Balears, I., Rosselló, C., De, U., Balears, I., Femenia, A., De, U., Balears, I., Simal, S., De, U., Balears, I., Eim, V. S., Rosselló, C., Femenia, A., & Simal, S. (2011). Moisture sorption isotherms and thermodynamic properties of carrot moisture sorption isotherms and thermodynamic properties of carrot. https://doi.org/10.2202/1556-3758.1804, 7, 3.

Fan, F., Mou, T., Nurhadi, B., & Roos, Y. H. (2017). Water sorption-induced crystallization, structural relaxations and strength analysis of relaxation times in amorphous lactose/whey protein systems. *Journal of Food Engineering, 196*, 150–158. https://doi.org/10.1016/j.jfoodeng.2016.10.022

Fan, K., Zhang, M., & Bhandari, B. (2019). Osmotic-ultrasound dehydration pretreatment improves moisture adsorption isotherms and water state of microwave-assisted vacuum fried purple-fleshed sweet potato slices. *Food and Bioproducts Processing, 115*, 154–164.

García-Alamilla, P., Lagunes-Gálvez, L. M., Barajas-Fernández, J., & García-Alamilla, R. (2017). Physicochemical changes of cocoa beans during roasting process. *Journal of Food Quality*. https://doi.org/10.1155/2017/2969324, 2017.

García-Pérez, J. V., Cárcel, J. A., Clemente, G., & Mulet, A. (2008). Water sorption isotherms for lemon peel at different temperatures and isosteric heats. *Lebensmittel-Wissenschaft und -Technologie- Food Science and Technology, 41*(1), 18–25. https://doi.org/10.1016/j.lwt.2007.02.010

Geeraert, L., Berecha, G., Honnay, O., & Aerts, R. (2019). Organoleptic quality of Ethiopian Arabica coffee deteriorates with increasing intensity of coffee forest management. *Journal of Environmental Management, 231*(May 2018), 282–288. https://doi.org/10.1016/j.jenvman.2018.10.037

Goneli, A. L. D., Corrêa, P. C., Oliveira, G. H. H., & Afonso Júnior, P. C. (2013). Water sorption properties of coffee fruits, pulped and green coffee. *Lebensmittel-Wissenschaft und -Technologie- Food Science and Technology, 50*(2), 386–391. https://doi.org/10.1016/j.lwt.2012.09.006

Hanson, A. B. (2022). *ChemoSpec: Exploratory chemometrics for spectroscopy*. R package version 6.1.0 https://CRAN.R-project.org/package=ChemoSpec.

Herman, C., Spreutels, L., Turomzsa, N., Konagano, E. M., & Haut, B. (2018). Convective drying of fermented Amazonian cocoa beans (Theobroma cacao var. Forasteiro). Experiments and mathematical modeling. *Food and Bioproducts Processing, 108*, 81–94. https://doi.org/10.1016/j.fbp.2018.01.002

Iaccheri, E., Laghi, L., Cevoli, C., Berardinelli, A., Ragni, L., Romani, S., & Rocculi, P. (2015). Different analytical approaches for the study of water features in green and roasted coffee beans. *Journal of Food Engineering, 146*, 28–35. https://doi.org/10.1016/j.jfoodeng.2014.08.016

Iaccheri, E., Ragni, L., Cevoli, C., Romani, S., Dalla Rosa, M., & Rocculi, P. (2019). Glass transition of green and roasted coffee investigated by calorimetric and dielectric techniques. *Food Chemistry, 301*(July), 125187. https://doi.org/10.1016/j.foodchem.2019.125187

Meza, B. E., Carboni, A. D., & Peralta, J. M. (2018). Food and Bioproducts Processing Water adsorption and rheological properties of full-fat and low-fat cocoa-based confectionery coatings. *Food and Bioproducts Processing, 110*, 16–25. https://doi.org/10.1016/j.fbp.2018.04.005

Mutlu, C., Candal-Uslu, C., Kılıç-Büyükkurt, Ö., & Erbaş, M. (2020). Sorption isotherms of coffee in different stages for producing Turkish coffee. *Journal of Food Processing and Preservation*, 1–7. https://doi.org/10.1111/jfpp.14440. August 2019.

de Oliveira, G. H. H., Corrêa, P. C., de Oliveira, R. L. A. P., Baptestini, M. F., & Vargas-Elías, A. G. (2016). Roasting, grinding, and storage impact on thermodynamic properties and adsorption. https://doi.org/10.1111/jfpp.12779, 1-12.

Özdestan, Ö., van Ruth, S. M., Alewijn, M., Koot, A., Romano, A., Cappellin, L., & Biasioli, F. (2013). Differentiation of specialty coffees by proton transfer reaction-mass spectrometry. *Food Research International, 53*(1), 433–439. https://doi.org/10.1016/j.foodres.2013.05.013

Rodríguez-Bernal, J. M., Flores-Andrade, E., Lizarazo-Morales, C., Bonilla, E., Pascual-Pineda, L. A., Gutierréz-López, G., & Quintanilla-Carvajal, M. X. (2015). Moisture adsorption isotherms of the borojó fruit (Borojoa patinoi. Cuatrecasas) and gum Arabic powders. *Food and Bioproducts Processing, 94*, 187–198. https://doi.org/10.1016/j.fbp.2015.03.004

Rojas, S. M., Chejne, F., Ciro, H., & Montoya, J. (2020). Roasting impact on the chemical and physical structure of Criollo cocoa variety (Theobroma cacao L). *Journal of Food Process Engineering*. https://doi.org/10.1111/jfpe.13400. May 2019.

Shittu, T. A., Idowu-adebayo, F., Adedokun, I. I., & Alade, O. (2015). Water vapor adsorption characteristics of starch À albumen powder and rheological behavior of its paste. *Nigerian Food Journal, 1*, 7. https://doi.org/10.1016/j.nifoj.2015.04.014

Sormoli, E. M., & Langrish, T. A. G. (2015). Moisture sorption isotherms and net isosteric heat of sorption for spray-dried pure orange juice powder. *Lebensmittel-Wissenschaft und -Technologie- Food Science and Technology, 62*(1), 875–882. https://doi.org/10.1016/j.lwt.2014.09.064

Tao, Y., Wu, Y., Yang, J., Jiang, N., Wang, Q., Chu, D., Han, Y., & Zhou, J. (2018). Thermodynamic sorption properties , water plasticizing effect and particle characteristics of blueberry powders produced from juices , fruits and pomaces. *Powder Technology, 323*, 208–218. https://doi.org/10.1016/j.powtec.2017.09.033

Tolessa, K., Rademaker, M., De Baets, B., & Boeckx, P. (2016). Prediction of specialty coffee cup quality based on near infrared spectra of green coffee beans. *Talanta, 150*, 367–374. https://doi.org/10.1016/j.talanta.2015.12.039

Tripetch, P., & Borompichaichartkul, C. (2019). Effect of packaging materials and storage time on changes of colour, phenolic content, chlorogenic acid and antioxidant activity in arabica green coffee beans (Coffea arabica L. cv. Catimor). *Journal of Stored Products Research, 84*, 101510. https://doi.org/10.1016/j.jspr.2019.101510

Velásquez, S., Franco, A. P., Peña, N., Bohórquez, J. C., & Gutierrez, N. (2021). Effect of coffee cherry maturity on the performance of the drying process of the bean: Sorption isotherms and dielectric spectroscopy. *Food Control, 123*, 1–8. https://doi.org/10.1016/j.foodcont.2020.107692. July 2020.

Velásquez, S., Peña, N., Bohórquez, J. C., Gutierrez, N., & Sacks, G. L. (2019). Volatile and sensory characterization of roast coffees – effects of cherry maturity. *Food Chemistry, 274*(May 2018), 137–145. https://doi.org/10.1016/j.foodchem.2018.08.127

Velázquez-Gutiérrez, S. K., Figueira, A. C., Rodríguez-Huezo, M. E., Román-Guerrero, A., Carrillo-Navas, H., & Pérez-Alonso, C. (2015). Sorption isotherms, thermodynamic properties and glass transition temperature of mucilage extracted from chia seeds (Salvia hispanica L.). *Carbohydrate Polymers, 121*, 411–419. https://doi.org/10.1016/j.carbpol.2014.11.068

Yao, K., Anthony, J., Maghirang, R., Hagstrum, D., Zhu, K. Y., & Bhadriraju, S. (2020). Using dynamic dewpoint isotherms to determine the optimal storage conditions of inert dust-treated hard red winter wheat. *Grain & Oil Science and Technology*. https://doi.org/10.1016/j.gaost.2020.06.004

Yogendrarajah, P., Samapundo, S., Devlieghere, F., De Saeger, S., & De Meulenaer, B. (2015). Moisture sorption isotherms and thermodynamic properties of whole black peppercorns (Piper nigrum L.). *Lebensmittel-Wissenschaft und -Technologie- Food Science and Technology, 64*(1), 177–188. https://doi.org/10.1016/j.lwt.2015.05.045